Tuning the Ferromagnetic Coupling of Fe Nanodots on Cu(111) via Dimensionality Variation of the Mediating Electrons

Lifeng Yin,[1,2] Di Xiao,[1] Zheng Gai,[1] Thomas Z. Ward,[1] Noppi Widjaja,[1,3] G. Malcolm Stocks,[1] Zhao-hua Cheng,[4]
E. Ward Plummer,[5] Zhenyu Zhang,[1,3] and Jian Shen[1,2,*]

[1]*Materials Science and Technology Division, Oak Ridge National Laboratory, Oak Ridge, Tennessee 37831, USA*
[2]*Department of Physics, Fudan University, Shanghai 200433, China*
[3]*Department of Physics & Astronomy, University of Tennessee, Knoxville, Tennessee 37996, USA*
[4]*Institute of Physics, Chinese Academy of Sciences, Beijing 100190, China*
[5]*Department of Physics & Astronomy, Louisiana State University, Baton Rouge, Louisiana 70803, USA*
(Received 19 October 2009; published 20 April 2010)

Using *in situ* magneto-optical Kerr effect measurements and phenomenological modeling, we study the tunability in both the magnetization anisotropy and magnetic coupling of Fe nanodots on a curved Cu(111) substrate with varying vicinity. We observe that, as the terrace width w decreases, the magnetization anisotropy increases monotonically, faster when w is smaller than the nanodot size d. In contrast, the magnetic coupling strength also increases until $w \sim d$, after which it decreases steeply. These striking observations can be rationalized by invoking the counterintuitive dimensionality variation of the surface electrons mediating the interdot coupling: the electrons are confined to be one dimensional (1D) when $w \gtrsim d$, but become quasi-2D when $w < d$ due to enhanced electron spillover across the steps bridged by the nanodots.

In low-dimensional materials, the interplay between quantum confinement and broken symmetry often leads to novel electronic and crystallographic structures. As a result, the corresponding physical properties can be changed dramatically on a macroscopic scale. Uncovering and exploiting these emergent phenomena relies critically on the ability to tune the dimensionality of the electronic structure within the materials; such research efforts are also vital for achieving enhanced functionality for future technological applications.

The pronounced two-dimensional (2D) surface states on Cu(111) have been shown to mediate a wide variety of fascinating quantum phenomena [1–6]. Further, it has been shown that these surface states can mediate the ferromagnetic coupling between randomly distributed Fe nanodots and give rise to 2D artificial magnets [7,8]. Compared to conventional magnets, such artificial magnets allow much easier tuning of nearest neighbor magnetic interactions (the dot-dot interactions). Investigating the artificial magnets formed by interacting nanodot assemblies will not only enrich our understanding of magnetism in nanomaterials [9], but also advance our capabilities to fabricate magnetic nanodot assemblies with tunable magnetic properties for future applications [10,11].

Recently, it was shown theoretically that a strong ferromagnetic coupling between Fe nanodots on Cu(111) can be realized if the nanodots are partially embedded into the Cu substrate [12]. In this Letter, we show that both the magnetic anisotropy and the ferromagnetic coupling of the Fe nanodot assemblies can be tuned by controlling the dimensionality of the Cu(111) surface states. This was achieved by growing the Fe nanodots on the vicinal surfaces where the terraces are confined by neighboring parallel aligned steps to allow 1D quantum-well states to form [13–17]. With increasing vicinal angle θ or decreasing terrace width w, we observed a striking nonmonotonic change of the magnetic coupling strength. The coupling strength first increases until the Fe nanodot size d equals w, then decreases steeply when $w < d$. This is surprising since the corresponding magnetic anisotropy is observed to increase monotonically as w decreases, and in fact, increases even faster when $w < d$. Based on our model calculations, we attribute the origin of this surprising observation to a counterintuitive dimensionality variation of the surface electrons mediating the interdot coupling: the surface electrons are confined to be 1D when $w \gtrsim d$, but become quasi-2D when they are further squeezed into narrower terraces ($w < d$) due to enhanced electron spillover across the steps bridged by the nanodots.

The Fe nanodot assemblies were grown using buffer layer assisted growth [18] in an ultrahigh vacuum (UHV) system with base pressures $<1 \times 10^{-10}$ Torr. A curved Cu(111) surface with a miscut angle ranging from 0.8° to 7.2° (miscut towards $[\bar{1}\,\bar{1}\,2]$ with {100} type steps [15]) was used as the substrate and consisted of terraces of continuously varying width down to 1.7 nm across the surface. The substrate was prepared by cycles of 1 keV Ne ion sputtering and annealing to 800 K, before it was cooled to about 30 K. Inert Xe gas (5N purity) was then released into the UHV chamber to form a solid buffer layer on top of the Cu substrate. Fe (5N purity) was evaporated from a crucible heated by *e*-beam bombardment. After Fe deposition, the

sample was slowly warmed to 300 K to desorb the Xe buffer layer and allow the Fe nanodots to softly land on the Cu substrate. The deposition rate was independently calibrated by Auger Electron spectroscopy (AES) and microbalance. The diameter d and the density ρ of the Fe nanodots can be controlled by both the Xe dosage and Fe thickness [7]. The magnetic properties were characterized by *in situ* magneto-optical Kerr effect (MOKE).

On the curved Cu(111) substrate, the Fe nanodot assemblies exhibit collective ferromagnetic stability across the entire surface. Figure 1(a) shows typical hysteresis loops of a Fe nanodot assembly ($d \sim 3.1$ nm, $\rho \sim 1.4 \times 10^4/\mu m^2$) measured from surface locations with large and small terrace width. Figure 1(b) shows the corresponding time-dependent remanent magnetization M_r. During the measurements, the dot assemblies were first demagnetized and then magnetized by an in-plane field (~ 1000 Oe) perpendicular to the steps at the time marked "on." After the removal of the field (marked "off"), the magnetization falls rapidly to the M_r level and remains constant thereafter. The stable M_r allows us to define the critical temperature T_c and use the T_c value as a measure of the coupling strength between the Fe nanodots.

The coupling strength of the Fe nanodots on the curved Cu(111) surface is found to depend strongly on the terrace width. Figure 2(a) shows the temperature dependent M_r/M_s ratio of the 3.1 nm Fe nanodot assembly measured at surface locations with several representative terrace widths. Interestingly, the T_c for $w = 3.1$ nm appears to be higher than those measured from both wider (14.9 nm) and narrower (1.7 nm) terraces. This nonmonotonic behavior is most evident in Fig. 2(b), which shows the T_c values as a function of the terrace width. Two regimes can be identified with a sharp transition at $w = d$: in regime I, T_c increases with decreasing w, from 210 K at $w = 14.9$ nm to 248 K at $w = 3.1$ nm; and in regime II (1.7 nm $< w <$ 3.1 nm), the T_c falls rapidly.

To understand the nonmonotonic behavior of T_c with changing w, we first investigate the magnetic anisotropy of the Fe nanodot assemblies. Similar to those on a flat Cu(111) surface [7], the Fe nanodot assemblies on the curved surface also exhibit an in-plane easy magnetization since no magnetization signal can be detected by polar MOKE (magnetic field perpendicular to the surface). Within the surface plane, however, the Fe nanodot assemblies on the curved surface show clear uniaxial anisotropy, in drastic contrast to the isotropic behavior of those on the flat surface. Figures 3(a) show longitudinal MOKE hysteresis loops of the 3.1 nm Fe nanodot assembly. As summarized in the inset of Fig. 3(b), the M_r/M_s ratio measured along the step direction is significantly larger than that measured in the orthogonal direction independent of the terrace width. This indicates in-plane uniaxial anisotropy with easy axis along the step direction.

The saturation field (H_s) determined from the hard axis magnetization loop can be used as a measure of the uniaxial anisotropy strength. Figure 3(b) shows the H_s of the 3.1 nm Fe nanodot assembly as a function of w. Again, two regimes can be distinguished. In regime I where $w > d$ (note that nanodots try to avoid contact with step edges unless they are forced to do so [7,19]), H_s shows a clear trend of increasing with decreasing w. Therefore, the 1D confinement results in an increase in the anisotropic strength, because the nanodots can "feel" the symmetry breaking through the surface states [20]. In regime II where $w < d$, H_s increases with a distinctly larger slope than in regime I. This rapid increase can be understood by the additional uniaxial anisotropy induced by the step edges. When $w < d$, each nanodot is *forced* to straddle across the step edges. The step edges further enhance the uniaxial anisotropy of each nanodot by the same mechanism that is commonly seen in magnetic thin films on vicinal surfaces [21,22]. Because the number of steps underneath the nanodot increases with decreasing terrace width in regime II, it leads to a more rapid increase in the uniaxial anisotropy.

In low-dimensional magnetic systems such as ultrathin films [23,24] and nanodots [25], in general, a larger anisotropy generally provides a larger energy barrier to compete against thermal fluctuations and thus results in a
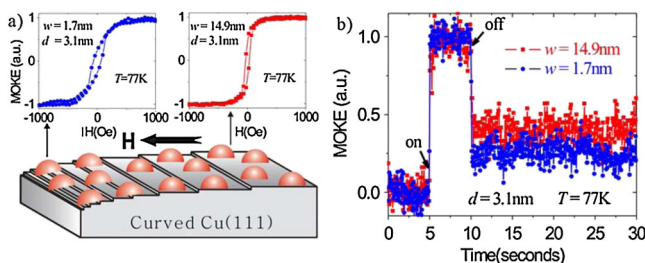

FIG. 1 (color online). (a) Illustration of the Fe dot assembly on a curved Cu substrate. The inset is typical hysteresis loops of Fe dot assemblies atop high miscut angle ($w = 1.7$ nm, $\theta = 7.2°$) and low miscut angle ($w = 14.9$ nm, $\theta = 0.8°$) positions. (b) The corresponding time-dependent M_r of the Fe dot assemblies. An in-plane external field was applied at the time marked "on," and then was switched off at the time marked "off."
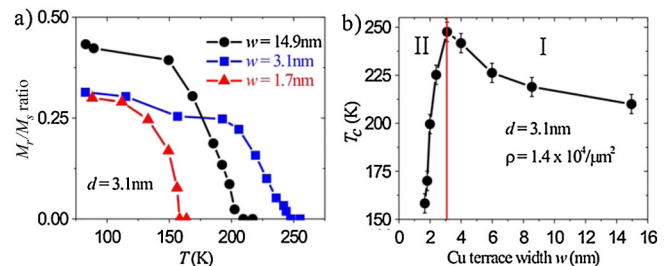

FIG. 2 (color online). (a) Temperature dependent M_r/M_s ratios of Fe dot assemblies with $d = 3.1$ nm measured on terrace widths of 14.9, 3.1, and 1.7 nm. The $w = 3.1$ nm curve shows the highest T_c. (b) T_c as a function of w shows a maximum where $w = d$. In regime I, T_c increases with decreasing w, from 210 K on the 14.9 nm terrace to 248 K on the 3.1 nm terrace; and in regime II, the T_c falls rapidly between the 3.1 nm and the 1.7 nm terrace width.
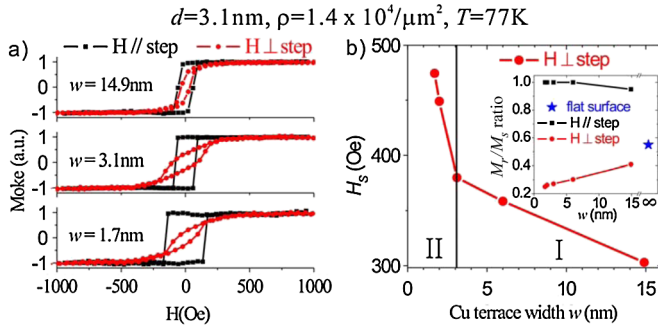
FIG. 3 (color online). (a) MOKE hysteresis loops of the Fe dot assemblies ($d = 3.1$ nm) on different terrace widths, $w = 14.9$, 3.1, and 1.7 nm, respectively. Note that all show a clear uniaxial anisotropy with easy axis along the step. (b) Summarized saturation field H_S as a function of w indicates an enhancement of anisotropy. The inset is M_r/M_s ratio of hard and easy axis of vicinal surfaces with star indicating a flat surface.

higher T_c. The increasing magnetic anisotropy as shown in Fig. 3(b), should contribute to the increase of T_c in regime I of Fig. 2(b). However, if the anisotropy is the main cause, we should see an even more rapid increase of T_c with decreasing w in regime II, which contradicts the experimental results. Therefore the magnetic anisotropy alone cannot explain the nonmonotonic behavior of T_c in the combined regime I + II.

In addition to the magnetic anisotropy, the dot-dot interaction can also significantly affect T_c. Ignatiev et al. [12] has shown that on Cu(111) the Fe dot-dot coupling depends sensitively on structural factors such as size, density, crystallographic structure, and partial embedding of nanodots into the substrate. However, while acknowledging the importance of the structural factors, we point out that these structural factors do not change appreciably with changing terrace width. This conclusion is based on both our STM studies of Fe dot distribution on terraces of different width [26], which confirms the uniformity of size and density of Fe nanodots, and the following rational arguments regarding the crystallographic structure and the dot embedment in the substrate. For the crystallographic structure, we argue that it is highly unlikely that the crystallographic structure will change with changing terrace width because the Fe dots have a relatively large size (~1000 atoms) and are first formed on the Xe buffer layer before they come in contact with the substrate. As for the embedding issue, although we do not have direct experimental evidence to prove that the Fe dots are indeed embedded in the copper surface layer, the paper by Ignatiev et al. [12], indicates that the Fe dots are likely already embedded in the Cu surface layer on large terraces. The embedding process does not likely change significantly with decreasing terrace width because the Fe nanodots are rather large and thus "immobile." Moreover, even if the terrace width plays a role, the step edges will only assist the embedding process, according to Ignatiev et al. [12], we should observe an enhanced T_c with decreasing terrace width [12]. This is

contradictory to our experimental observation. Therefore, we conclude that there is no significant variation of embedding process upon changing of terrace width.

While not disturbing the structural factors of the Fe nanodots, the changing terrace width should make substantial modification to the nature of the surface states which would likely lead to a significant change in the observed T_c. Let us consider the evolution of the surface states as a function of w. At large values ($w \gtrsim d$), the surface states are confined by the terrace and form an array of 1D quantum-well states. In this regime, the deposited nanodots try to avoid contact with the step edges. As w shrinks to $w < d$, the nanodots are forced to sit on top of step edges, and as a result, they effectively couple the surface states of neighboring terraces, causing a transition of the surface states from 1D quantum-well states to quasi-2D.

Once we realize the dramatic difference associated with the dimensionality change induced by the nanodots, we can focus on the two regimes separately. When the system is in the 1D regime, the indirect exchange interaction decays as $1/R$ [27]. As w decreases further, the system enters the 2D regime, where the exchange interaction decays as $1/R^2$ for an isotropic Fermi surface [28]. Since the distance R between the nanodots is fixed, the sudden change in dimensionality of the surface states leads to the sharp drop in the T_c.

To calculate the RKKY interaction, one needs to know the energy spectra and wave functions of the electrons. One implication comes from the fact that the Fe nanodots are randomly located on the substrate, which requires the diagonalization of a rather complicated Hamiltonian. Since our focus is on the dimensionality change, we choose to consider a "clean" system where there is a periodic coupling between the surface electrons on neighboring terraces, as the RKKY range function is essentially unaffected by weak disorder [29]. The energy spectrum of the surface states thus takes the following form:

$$E_k = \frac{\hbar^2}{2m}\left[k_x^2 + \left(\frac{\pi}{w}\right)^2\right] - \lambda \cos k_y w. \tag{1}$$

Here the x axis is along the steps and the y axis perpendicular to the steps. The first term comes from the fact that the electrons can freely move along the step direction and are confined by the steps in the y direction [13], and the second term represents the weak coupling of surface states on neighboring terraces, with λ measuring the coupling strength. $\lambda = 0$ for $w \gtrsim d$ (corresponding to 1D surface states) and increases with shrinking w when $w < d$. We consider the situation where w is small enough so that only the lowest subband is populated. In addition to the 1D to 2D transition, reducing w also raises the band bottom of the surface states thus gradually depopulating the surface states. Given the energy spectra in Eq. (1), the exchange interaction can then be calculated according to the standard RKKY theory [27,28,30]. The configuration-averaged exchange interaction $J_{\text{eff}} = \int d\vec{r} J^{\text{RKKY}}(\vec{r})$ as a function of w
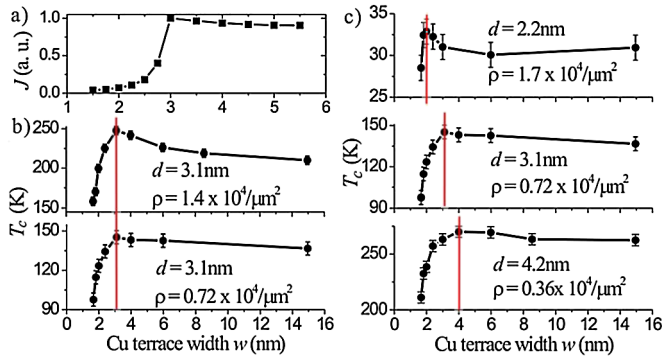
FIG. 4 (color online). (a) Exchange interaction strength as a function of the terrace width obtained from a phenomenological model of surface-state mediated dot-dot coupling. The parameters used in the calculations correspond to the case where $d = 3.1$ nm and $\rho = 1.4 \times 10^4/\mu m^2$. (b) Density comparison of Fe dot assembles with dot size of 3.1 nm—note that both have maximum T_c at the same terrace width. (c) Terrace width dependence on T_c values for Fe dot assemblies of dot size of 2.2, 3.1, and 4.2 nm. The maximum T_c is always located at where $w = d$.

is shown in Fig. 4(a), with $\lambda = 0.01 \frac{\hbar^2}{w^2 m} \frac{d-w}{d}$. It is clear that the exchange interaction behaves differently in the two regimes. In regime I ($w \geq d$), the slight increase of the exchange interaction towards $w = d$ is due to the enhanced confinement with reduced w, originating from the characteristic form of the RKKY interaction in 1D [27]. The sharp drop in regime II ($w < d$) is due to the transition into the quasi-2D case, where the interaction decays as $1/R^2$ instead of $1/R$ [27,28]. As w continues decreasing to $\sim \lambda_F/2$, the surface states are completely depopulated, leading to a vanishing exchange interaction [31]. The closely matching trend of the exchange interaction from the model calculations and the observed T_c strongly suggest that the nanodot induced dimensionality change is the main mechanism responsible for the nonmonotonic behavior of T_c.

If our argument holds, T_c should show a similar dependence on the terrace width for Fe nanodot assemblies having different size and density, i.e., reaching the maximum only when $w = d$. As shown in Fig. 4, this is indeed the case. We first compare two Fe nanodot assemblies of the same size but different density in Fig. 4(b). Apparently, both the T_c values peak at the same point. This occurs despite the fact that the T_c of the low-density nanodot assembly is considerably lower than that of the high-density one. Figure 4(c) again shows that the T_c of nanodot assemblies with different size all peak at the point where $w = d$. These crosschecks corroborate the overall physical interpretation reached from the phenomenological model.

In summary, we have demonstrated intriguing tunability in both the magnetic anisotropy and the ferromagnetic coupling strength of the Fe nanodot assemblies on vicinal Cu(111). We have further identified the nanodot induced dimensionality change of the surface-state electrons as the

main mechanism responsible for the nonmonotonic behavior of T_c. These electrons are confined to be 1D when $w \geq d$, but become quasi-2D when $w < d$ due to enhanced electron spillover across the steps bridged by the straddling nanodots.

*To whom correspondence should be addressed.
shenj@ornl.gov
[1] M. F. Crommie et al., Science **262**, 218 (1993).
[2] H. C. Manoharan et al., Nature (London) **403**, 512 (2000).
[3] V. S. Stepanyuk et al., Phys. Rev. Lett. **94**, 187201 (2005).
[4] J. Merino and O. Gunnarsson, Phys. Rev. Lett. **93**, 156601 (2004).
[5] J. Repp et al., Phys. Rev. Lett. **85**, 2981 (2000).
[6] V. S. Stepanyuk et al., Phys. Rev. B **68**, 205410 (2003).
[7] J. P. Pierce et al., Phys. Rev. Lett. **92**, 237201 (2004).
[8] M. A. Torija et al., Phys. Rev. Lett. **95**, 257203 (2005).
[9] R. F. Wang et al., Nature (London) **439**, 303 (2006).
[10] Shouheng Sun et al., Science **287**, 1989 (2000).
[11] C. T. Black et al., Science **290**, 1131 (2000).
[12] P. A. Ignatiev et al., Phys. Rev. B **80**, 165408 (2009).
[13] L. Bürgi et al., Phys. Rev. Lett. **81**, 5370 (1998).
[14] F. Baumberger et al., Phys. Rev. Lett. **92**, 196805 (2004).
[15] A. Mugarza et al., J. Phys. Condens. Matter **18**, S27 (2006).
[16] J. E. Ortega et al., Phys. Rev. Lett. **84**, 6110 (2000).
[17] F. Baumberger et al., Phys. Rev. Lett. **92**, 016803 (2004).
[18] L. Huang, S. J. Chey, and J. H. Weaver, Phys. Rev. Lett. **80**, 4095 (1998).
[19] J. Zhang et al., Eur. Phys. J. D **45**, 515 (2007).
[20] L. Szunyogh et al., Phys. Rev. Lett. **96**, 067204 (2006).
[21] D. S. Chuang, C. A. Ballentine, and R. C. O'Handley, Phys. Rev. B **49**, 15 084 (1994).
[22] Y. Z. Wu, C. Won, and Z. Q. Qiu, Phys. Rev. B **65**, 184419 (2002).
[23] Hyuk J. Choi et al., Phys. Rev. Lett. **82**, 1947 (1999).
[24] R. Cheng, S. D. Bader, and F. Y. Fradin, Phys. Rev. B **77**, 024404 (2008).
[25] L. Wang et al., Phys. Rev. B **64**, 214410 (2001).
[26] See supplementary material at http://link.aps.org/supplemental/10.1103/PhysRevLett.104.167202 for details.
[27] Y. Yafet, Phys. Rev. B **36**, 3948 (1987).
[28] B. Fischer and M. W. Klein, Phys. Rev. B **11**, 2025 (1975).
[29] A. Yu. Zuzin and B. Z. Spivak, JETP Lett. **43**, 234 (1986); L. N. Bulaevskii and S. V. Panyukov, JETP Lett. **43**, 240 (1986); A. Jagannathan, E. Abrahams, and M. J. Stephen, Phys. Rev. B **37**, 436 (1988).
[30] M. A. Ruderman and C. Kittel, Phys. Rev. **96**, 99 (1954); T. Kasuya, Prog. Theor. Phys. **16**, 45 (1956); K. Yosida, Phys. Rev. **106**, 893 (1957).
[31] K. Morgenstern, K. F. Braun, and K. H. Rieder, Phys. Rev. Lett. **89**, 226801 (2002).